

# New types of liquid crystalline epoxy resins cured by a mesogenic hardening compound

Shunichi Osada and Shinichi Yano\*

*Department of Chemistry, Faculty of Engineering, Gifu University, 1-1 Yanagido, Gifu 501-11, Japan*

and Kenji Tsunashima\*

*Films and Film Products Research Laboratories, Toray Industries Inc., 1-1 Sonoyama 1-chome, Otsu, Shiga 520, Japan*

and Toshihide Inoue

*Plastic Research Laboratories, Toray Industries Inc., 9-1 Oe-Cho, Minato-Ku, Nagoya 455, Japan*

*(Received 11 August 1995; revised 19 September 1995)*

The new epoxy resins, EPD-CAA10 and EPTB-CAA10, were synthesized by reacting stoichiometrically the diepoxides, 4,4'-bis(2,3-epoxypropoxy)bisphenol A (EPB) and 4,4'-bis-2,3-epoxypropoxy)-3,3',5,5'-tetramethylbiphenol (EPTB), respectively, with a mesogenic hardening compound, 4,4'-bis( $\omega$ -carboxydecanoxy)azoxybenzene (CAA10), using tri-*n*-butylamine as a catalyst. The reaction procedures and the mesogenic phase transitions for the two epoxy resins were studied by the use of infra-red (i.r.), spectroscopy, differential scanning calorimetry (d.s.c.) polarizing microscopy and X-ray diffraction spectroscopy. It was found that both of the differential EPB-CAA10 and EPTB-CAA10 systems had a mesophase which was functionalized by the mesogenic hardening compound; EPB-CAA10 showed a smectic-like mesophase between 70 and 90°C when the polymer was not gelled but had no mesophase when gelled, while EPTB-CAA10 also had a smectic-like mesophase when not gelled, but showed a nematic phase when gelled. Copyright © 1996 Published by Elsevier Science Ltd.

**(Keywords: liquid crystal; epoxy resin; mesogenic hardening compounds)**

## INTRODUCTION

Recently, scientific and industrial interest in liquid crystalline thermosetting resins (LCTs) has been increasing<sup>1–13</sup>, due to the fact that these materials can offer characteristic properties which can be modified by the outstanding properties of liquid crystalline (LC) polymers. As is well known, epoxy resins are one of the most important classes of thermosetting engineering plastics and have been widely used because of their characteristic properties such as strong bonding strength, high insulation resistance, and good thermal, oil and chemical resistances<sup>14</sup>. Recently, a number of LC epoxy resins have been synthesized and their physical and mesomorphic properties studied<sup>4–13</sup>; the LC diepoxides were synthesized and then polymerized by using commercial organic amines as hardening agents. Some of the epoxy resins produced showed mesomorphic states, and their mesophases were sometimes locked in the network matrix, when the resins were fully crosslinked by hardening. Other work has been devoted to the photoinitiated polymerization of LC diepoxides with organic amines. In such studies a mixture of LC diepoxide monomer and organic amine was uniformly

oriented on a glass plate and then polymerized under u.v. light. The polymer sheets that were obtained generally retained an oriented arrangement of the monomer mixture in the network structure and so were anisotropic. In this previous work, mesogenic diepoxide monomers have been used as key compounds for obtaining LC epoxy resins, but mesogenic hardening compounds have not been used to our knowledge. We believe that the use of mesogenic hardening compounds provides a new way to obtain useful LC epoxy resins, because it is possible to design a characteristic LC epoxy resin by choosing an appropriate hardening compound whose properties, e.g. acidity/basicity, reactivity with epoxide, and mesogenicity, should be associated with the chemical structure. Very recently, we have preliminarily reported a new type of LC epoxy resin cured by the mesogenic hardening compound, 4,4'-bis( $\omega$ -carboxydecanoxy)azoxybenzene (CAA10)<sup>13</sup>. This preliminary work has stimulated us to carry out further studies on LC epoxy resins cured with various other mesogenic hardening compounds. This present work has been undertaken in order to develop a new class of LC epoxy resins cured by the use of mesogenic hardening compounds. The chemical structures of the monomers used here are listed in *Figure 1*. The reaction mechanisms, mesomorphic phase transitions and physical

\* To whom correspondence should be addressed

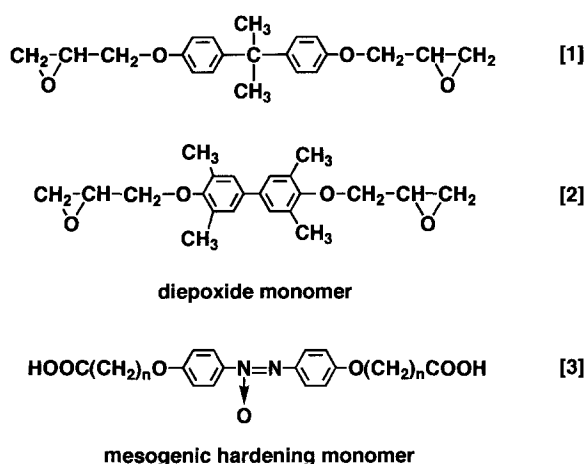


**Figure 1** Chemical structures of the two diepoxides and the mesogenic hardening monomers: (1) 4,4'-bis(2,3-epoxypropoxy)bisphenol A (EPB); (2) 4,4'-bis(2,3-epoxypropoxy)-3,3',5,5'-tetramethylbiphenol (EPTB); (3) 4,4'-bis( $\omega$ -carboxyalkoxy)azoxybenzenes (CAA<sub>n</sub>), where *n* is the number of CH<sub>2</sub> units in the alkoxy group

properties have been investigated for the new LC epoxy resins that have been obtained.

## EXPERIMENTAL

4,4'-Dihydroxyazoxybenzene was prepared by stirring *p*-nitrophenol (25.0 g, 203 ml) and benzene sulfonyl chloride (26.0 g, 151 ml) in pyridine (175 ml) for 12 h at 25°C, followed by a further 1 h at ~90°C. The solution was acidified by adding 25% H<sub>2</sub>SO<sub>4</sub> and the crude product was then extracted with ether. The crude crystals that were obtained were recrystallized from 50% ethanol after washing with benzene, giving yellow needle-like crystals (yield = 43.7%). 4,4'-Bis( $\omega$ -ethoxycarboxyalkoxy)azoxybenzenes (ECA<sub>n</sub>), where *n* is the number of CH<sub>2</sub> units in the alkoxy group) were synthesized by a Williamson reaction between 4,4'-dihydroxyazoxybenzene and the appropriate ethyl- $\omega$ -bromoalkanoate, while the 4,4'-bis( $\omega$ -carboxyalkoxy)azoxybenzenes (CAA<sub>n</sub>) were obtained by hydrolysing the corresponding ECA<sub>n</sub> compound. The specific preparative procedure for 4,4'-bis( $\omega$ -carboxydecanoxy)azoxybenzene (CAA10) is given as follows. A solution of 4,4'-dihydroxyazoxybenzene (13.42 g 58.3 mmol) and *t*-butoxypotassium (19.63 g, 175 mmol) in ethanol (200 ml) was added dropwise to ethyl 11-bromodecanoate (119.65 g, 408 mmol) in ethanol (80 ml), and refluxed for 24 h. The crude ECA10 crystals were recrystallized from ethanol after washing with water, giving yellow needle-like crystals (yield = 69%). CAA10 was obtained by refluxing EAA10 (26.29 g, 40.20 mmol) and NaOH (15.78 g, 281 mmol) in 75% ethanol (800 ml) for 12 h. The crude crystals that were obtained were recrystallized from 90% acetic acid solution, giving yellow crystalline needles (yield = 87.5%). The CAA10 crystals obtained were judged to be thoroughly pure from elemental analyses, and nuclear magnetic resonance (n.m.r.) and i.r. spectroscopy.

<sup>1</sup>H n.m.r.(DMSO)-d<sub>6</sub>  $\delta$ : 1.25–1.50 (m, CH<sub>2</sub>, 28H), 1.67–1.78 (m,  $\beta$ -C in decanoxy, 4H), 2.18 (t,  $\alpha$ -C in carboxylate  $J = 7.0$  Hz, 4H), 4.07–4.10 (m,  $\alpha$ -C in carboxylate, 4H), 7.35 (t benzene,  $J = 8.6$  Hz, 4H), 8.19 (t benzene,  $J = 9.5$  Hz, 4H), and 11.8–12.3 (m, COOH).

Elemental analysis: found; C 68.04, H 8.53, N 4.47%; calculated; C 68.20, H 8.42, N 4.68%.

The diepoxide monomers used in this work were 4,4'-bis(2,3-epoxypropoxy) bisphenol A (Showa-Shell Co., EPON 925) (EPB) and 4,4'-bis(2,3-epoxypropoxy)-3,3',5,5'-tetramethylbiphenyl (Showa-Shell Co., YX4000) (EPTB), with equivalent epoxide values of 172–178 and 195 equiv. <sup>-1</sup>g, respectively.

The EPB and EPTB diepoxides were reacted, respectively, with the CAA10 hardening monomer in a Teflon beaker for ~10 min at 145°C, using tri-butylamine (TBA) as a catalyst, at an equivalent ratio of EPB/EPTB to CAA10 of 1/1; the amount of TBA added was ~3 mol% (with respect to CAA10). In these experiments, only CAA10 was used as the hardening monomer. The EPB-CAA10 and EPTB-CAA10 polymers thus obtained were used as 'prepolymers' in subsequent experiments.

Infra-red spectra were recorded by using a Perkin Elmer FT-IR 1640 spectrometer. The prepolymer, sandwiched between two KBr plates, was set in an OMRON heating cell which has temperature controlled with an OMRON E5T controller. The prepolymer in the KBr plates was first heated to 140°C over a period of ~15 min and the i.r. spectra were then measured as a function of the curing time at 140°C.

The thermal properties were measured by the use of a differential scanning calorimeter (Seiko-Denshi Co., SSC-5000) operating at a heating/cooling rate of 5°C min<sup>-1</sup> for EPB, EPTB and CAA10, and at 10°C min<sup>-1</sup> for the EPB-CAA10 and EPTB-CAA10 polymers. The texture of the liquid crystalline phases was examined by an optical microscopy (Nikon Optiphoto-Pol, XTP-11) equipped with a Mettler FP82 hot-stage, at a heating/cooling rate of 5°C min<sup>-1</sup>.

X-ray diffraction measurements were carried out with a Rigaku Denki RU200 diffractometer, using monochromatic CuK $\alpha$  radiation (50 kV, 200 mA), with the X-ray scattering intensities being detected by a scintillation counter incorporating a pulse-height analyser. Thermal expansion was measured at a heating rate of ~0.5°C min<sup>-1</sup> by the use of a glass capillary dilatometer (0.6 mm i.d.). The sample was carefully immersed in liquid mercury *in vacuo* in order to avoid the formation of voids on the surface of the sample, and the volume change of the sample with temperature was calculated from a reading of the height of mercury in the dilatometer capillary.

## RESULTS AND DISCUSSION

### Mesogenicity of the CAA<sub>n</sub> monomers

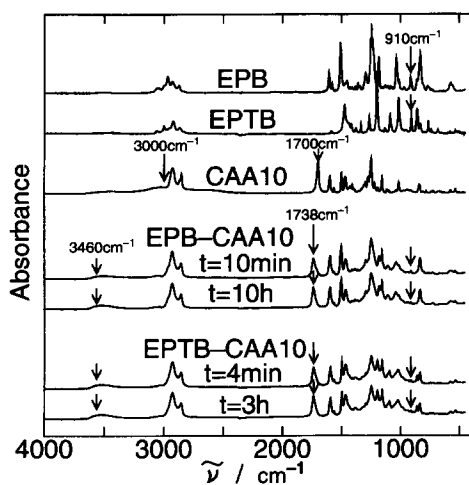
Mesomorphic phase transitions were studied for the homologous series of 4,4'-bis( $\omega$ -carboxyalkoxy)azoxybenzenes (CAA<sub>n</sub>) and their corresponding ethyl esters, i.e. 4,4'-bis( $\omega$ -ethylcarboxyalkoxy)azoxy benzenes (ECA<sub>n</sub>), by the use of d.s.c. and polarizing optical microscopy. The phase transition temperatures and the corresponding enthalpy changes are listed in Table 1. The CAA<sub>n</sub> homologues have no mesophase, but the ECAA<sub>n</sub> homologues have a smectic C (S<sub>c</sub>) phase when *n*  $\geq$  5. The ECAA5 compound shows a S<sub>c</sub> phase between 73 and 81°C and a nematic phase between 81 and 89°C, while compounds ECAA7 and ECAA10 show only a S<sub>c</sub> phase. The existence of ethylcarboxylate at the  $\omega$ -position decreases the thermal stability of the mesophase

**Table 1** Phase transition temperatures and corresponding enthalpy changes for 4,4'-bis( $\omega$ -carboxyalkoxy)azoxybenzenes (CAA $n$ ) and 4,4'-bis( $\omega$ -ethylcarboxyalkoxy)azoxybenzenes (ECAA $n$ )<sup>a</sup>

Class of compound	$n^b$	$K_1$	$K_2$	Smectic C	Nematic	Isotropic
CAA	3	• 183(10)	• 235(50)	–	–	•
	4	–	• 180(67)	–	–	•
	5	–	• 236(81)	–	–	•
	7	– 150(23)	• 216(75)	–	–	•
	10	•	• 157(74)	–	–	•
ECAA	1	• 108(6)	• 113(44)	–	–	•
	3	–	• 109(55)	–	–	•
	4	–	• 107(70)	–	–	•
	5	–	• 73(45)	• 81(2)	• 89(1)	•
	7	• 73(2)	• 83(45)	• 93(9)	–	•
	10	–	• 65(59)	• 88(13)	–	•

<sup>a</sup>  $K_1$  and  $K_2$  represent crystals 1 and 2, respectively, with the figures in the table being the phase transition temperatures ( $^{\circ}\text{C}$ ), with enthalpy changes ( $\text{kJ mol}^{-1}$ ) shown in parentheses

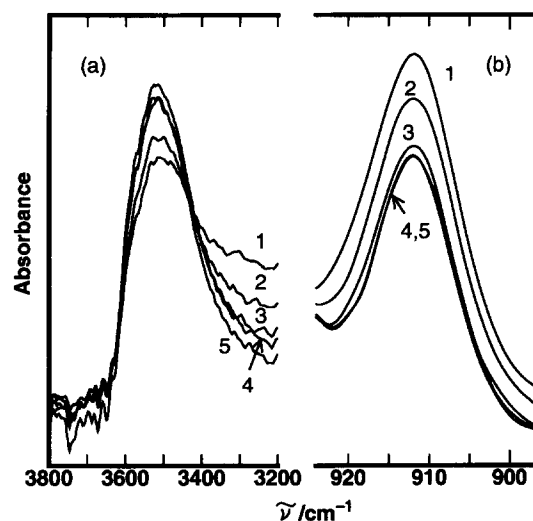
<sup>b</sup> Number of  $\text{CM}_2$  units in alkoxy group


**Figure 2** I.r. spectra of the EPB, EPTB, and CAA10 monomers, and EPB-CAA10 and EPTB-CAA10 polymers

much more in the ECAA $n$  homologues, compared with that in  $p,p'$ -alkoxyazoxybenzenes, ( $\text{C}_n\text{H}_{2n+1}\text{O}-\phi-\text{N}=\text{N}(\text{O})-\phi-\text{C}_n\text{H}_{2n+1}$ ) (PAA); for example, the  $n=3$  PAA homologue shows a nematic phase between 116 and  $123^{\circ}\text{C}$ , while the  $n=10$  homologue has a nematic phase between 78 and  $121^{\circ}\text{C}$  and a smectic phase between 121 and  $123^{\circ}\text{C}$ . Consequently, this present work indicates that the ECAA $n$  homologues are certainly mesogenic compounds, and that the CAA $n$  homologues can act as mesogenic hardening agents for epoxy resins<sup>15</sup>.

#### Study of hardening reaction mechanism by i.r. spectroscopy

Figure 2 shows i.r. spectra of the EPB, EPTB and CAA10 monomers, and the EPB-CAA10 and EPTB-CAA10 polymers. The CAA10 monomer shows two characteristic peaks near 1700 and  $3000\text{ cm}^{-1}$  which are attributed to the  $\text{C}=\text{O}$  ( $\nu_{\text{COOH}}(\text{C}=\text{O})$ ) and  $\text{OH}$  ( $\nu_{\text{COOH}}(\text{OH})$ ) stretching vibrations of the  $\text{COOH}$  group, respectively, while the EPB and EPTB monomers exhibit an antisymmetric stretching vibration of  $\text{C}-\text{C}$  in the epoxy ring near  $910\text{ cm}^{-1}$  ( $\nu(\text{C}-\text{C})$ ). These


**Figure 3** Variation of (a)  $\nu(\text{OH})$  at  $3460\text{ cm}^{-1}$  and (b)  $\nu(\text{C}-\text{C})$  at  $910\text{ cm}^{-1}$  with curing time ( $t$ ) for the EPB-CAA10 polymer: (1) 10; (2) 20; (3) 60; (4) 180; (5) 600 min

characteristic peaks significantly change by the hardening reaction of the EPB/EPTB diepoxides with CAA10. In the spectra of both EPB-CAA10 and EPTB-CAA10, where  $t$  represents the curing time at  $140^{\circ}\text{C}$ , the 910, 1700 and  $3000\text{ cm}^{-1}$  peaks are suppressed and new peaks appear near 1738 and  $3460\text{ cm}^{-1}$ , which are attributed, respectively, to the  $\text{C}=\text{O}$  vibration of the ester group ( $\nu_{\text{ester}}(\text{C}=\text{O})$ ) and the stretching vibration of the  $\text{OH}$  group ( $\nu(\text{OH})$ ) produced by a ring opening reaction of the epoxy group. These i.r. data indicate that the hardening reaction advances considerably, even after only 10 min of cure at  $140^{\circ}\text{C}$ . Figure 3 shows the variation of (a)  $\nu(\text{OH})$  near  $3460\text{ cm}^{-1}$  and (b)  $\nu(\text{C}-\text{C})$  near  $910\text{ cm}^{-1}$ , with  $t$  for EPB-CAA10, where both of the  $\nu(\text{OH})$  and  $\nu(\text{C}-\text{C})$  peaks are normalized by division by the height of the  $\text{C}=\text{C}$  stretching peak of benzene at  $1597\text{ cm}^{-1}$ . As the EPB-CAA10 and EPTB-CAA10 prepolymers become cured, the  $\nu(\text{OH})$  peak gradually increases, while the  $\nu(\text{C}-\text{C})$  peak decreases. Figure 4a shows how the  $\nu_{\text{ester}}(\text{C}=\text{O})$  peak changes with  $t$ , in which the  $\text{C}=\text{O}$  peak is also normalized by the  $\text{C}=\text{C}$  benzene

band at  $1597\text{ cm}^{-1}$ . Clearly, the  $\nu_{\text{ester}}(\text{C}=\text{O})$  peak is seen near  $1738\text{ cm}^{-1}$ , but the  $\nu_{\text{COOH}}(\text{C}=\text{O})$  band still remains near  $1700\text{ cm}^{-1}$ . As  $t$  increases, the  $\nu_{\text{ester}}(\text{C}=\text{O})$  peak gradually increases, while the  $\nu_{\text{COOH}}(\text{C}=\text{O})$  decreases, showing an isosbestic point (indicated by an arrow in the figure).

The existence of an isosbestic point indicates that the C=O peak for the COOH dimer is gradually replaced by that of the ester, as the prepolymer is cured at  $140^\circ\text{C}$ . We attempted to split the two C=O peaks by using the Monte Carlo method as proposed by Ivanov *et al.*<sup>16</sup>. We assume a function for the C=O spectrum ( $f_i$ ) as follows:

$$f_i = I_i [\exp(-(\nu_i - \nu_{i0})^2 / B_i^2) / (1.0 + 2.5(\nu_i - \nu_{i0}) / B_i)] \quad (1)$$

where  $\nu_i$ ,  $\nu_{i0}$ ,  $B_i$  and  $I_i$  are the wave number, wave number at the peak top, band width, and peak intensity for  $i$ th component, respectively.

We denoted  $i = 1$  and  $2$  for the  $\nu_{\text{ester}}(\text{C}=\text{O})$  and  $\nu_{\text{COOH}}(\text{C}=\text{O})$  peaks, respectively, and chose the parameters in order to minimize the difference between the experimental and calculated values during repeating of the calculations more than 2000 times. An example of a split i.r. spectrum is illustrated in Figure 5 for the

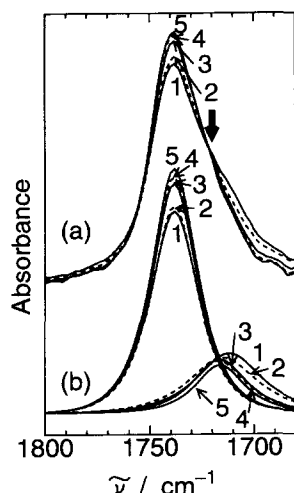


Figure 4 Variation of the C=O peak with curing time ( $t$ ) for EPB-CAA10, showing (a) experimental data for the C=O vibration, and (b) the split spectra,  $\nu_{\text{ester}}(\text{C}=\text{O})$  near  $1738\text{ cm}^{-1}$  and  $\nu_{\text{COOH}}(\text{C}=\text{O})$  near  $1710\text{ cm}^{-1}$ : (1) 10; (2) 20; (3) 60; (4) 180; (5) 600 min

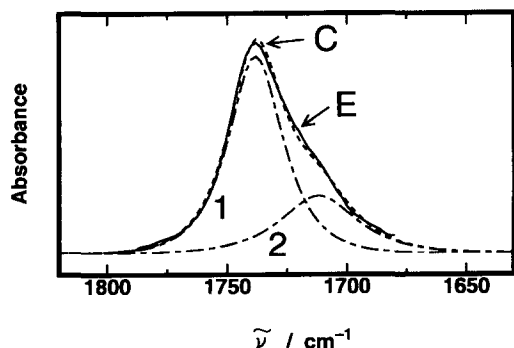


Figure 5 An example of splitting of the C=O peak into the  $\nu_{\text{ester}}(\text{C}=\text{O})$  and  $\nu_{\text{COOH}}(\text{C}=\text{O})$  components for EPB-CAA10 ( $t = 10\text{ min}$ ) by use of the Monte Carlo method<sup>16</sup>: (E) experimental data; (1) calculated  $\nu_{\text{ester}}(\text{C}=\text{O})$  curve; (2) calculated  $\nu_{\text{COOH}}(\text{C}=\text{O})$  curve; (C) calculated curves (the sum of 1 and 2)

EPB-CAA10 polymer cured for 10 min at  $140^\circ\text{C}$ . The calculated i.r. spectrum is well fitted to the experimental spectrum (error = ca. 1.6%) and therefore the split i.r. curves are judged to be reliable. In Figure 4b, we demonstrate how the split  $\nu_{\text{ester}}(\text{C}=\text{O})$  and  $\nu_{\text{COOH}}(\text{C}=\text{O})$  peaks change with  $t$ . As the EPB-CAA10 prepolymer is cured, the  $\nu_{\text{COOH}}(\text{C}=\text{O})$  peak decreases while the  $\nu_{\text{ester}}(\text{C}=\text{O})$  peak increases.

We have determined two reaction conversions, one by dividing the peak area of  $\nu_{\text{COOH}}(\text{C}=\text{O})$  with that of the unreacted mixture, and the other by dividing the peak area of  $\nu(\text{C}-\text{C})$  with that of the same mixture. All peak areas are normalized by using the area of the C=C stretching peak of benzene, as before. The unreacted mixture was prepared in the following way. EPB/EPTB, CAA10 and TNB were dissolved in THF in the same mixture ratio as that of the prepolymer, and the THF solvent is then evaporated from the solution and the remaining soil dried fully *in vacuo*. The i.r. spectra were measured for the dried mixture by the use of the KBr method. We used the normalized areas of the  $\nu_{\text{COOH}}(\text{C}=\text{O})$  and  $\nu(\text{C}-\text{C})$  peaks as the peak areas of the unreacted mixture, where we assume that the molar extinction coefficient is unchanged by the reaction. Figure 6 shows plots of the conversions, obtained from  $\nu_{\text{COOH}}(\text{C}=\text{O})$  and  $\nu(\text{C}-\text{C})$ , versus curing time ( $t$ ) at  $140^\circ\text{C}$  for the (a) EPB-CAA10 and (b) EPTB-CAA10 prepolymers. Both conversions increase rapidly with increasing  $t$  and saturate at  $\sim 200\text{ min}$  for EPB-CAA10 and at  $\sim 60\text{ min}$  for EPTB-CAA10. This saturation time is considered to represent the gelling time ( $t_g$ ) of the polymer. The saturated conversions from the  $\nu(\text{C}-\text{C})$  peak (reaction of the diepoxide) and  $\nu_{\text{COOH}}(\text{C}=\text{O})$  peak (reaction of COOH) were estimated to be  $\sim 83$  and  $75\%$ , respectively, for EPB-CAA10, and  $\sim 87$  and  $83\%$ , respectively, for EPTB-CAA10.

The value of the saturated conversion and its difference between  $\nu(\text{C}-\text{C})$  and  $\nu_{\text{COOH}}(\text{C}=\text{O})$  may be connected with the existence of a side reaction of the epoxide with the OH group. According to Alvey's study<sup>17</sup> of the reaction of EPB with adipic acid and its reaction mechanism, the

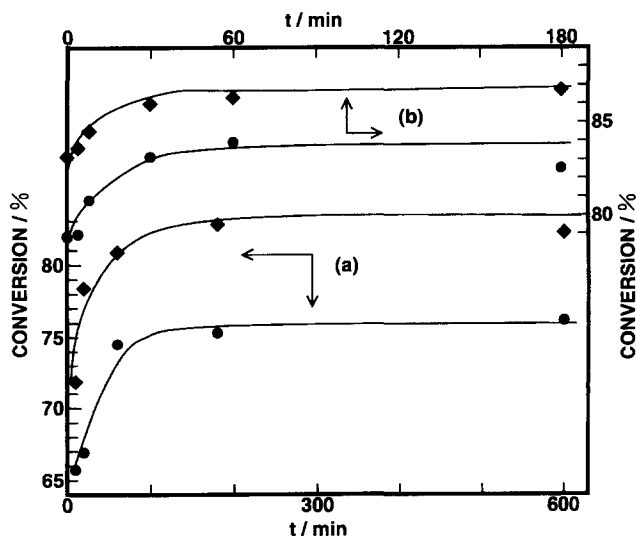


Figure 6 Plots of conversion (%) versus curing time ( $t$ ) at  $140^\circ\text{C}$  for (a) EPB-CAA10 and (b) EPTB-CAA10, using data calculated from: (●)  $\nu_{\text{COOH}}(\text{C}=\text{O})$ ; (◆)  $\nu(\text{C}-\text{C})$

hardening reaction propagates via two routes, namely the main reaction of the epoxide with COOH, and a side reaction, i.e. an etherification of the epoxide and OH groups produced by the main reaction. The TBA catalyst is known to 'prefer' the main reaction to the side reaction. The latter reaction of the epoxide with the OH groups produces interchain crosslinks and finally leads to gelation which would hinder the overall reaction. When  $t = t_g$ , the degree of branching (side reaction) was estimated to be ~8% for EPB-CAA10 and ~6% for EPTB-CAA10, from the following relationship:

$$\begin{aligned} \text{degree of branching} &= (\text{binding no. of etherification} \\ &\quad \text{of epoxide with the OH group}) / \\ &\quad (\text{binding no. of esterification} + \\ &\quad \text{bonding no. of etherification}) \\ &= (\text{conversion of epoxide} - \\ &\quad \text{conversion of COOH}) / \\ &\quad (\text{conversion of epoxide}) \end{aligned} \quad (2)$$

The degree of branching should correspond to the crosslink density. Assuming that all of the side reactions are those of the epoxide with the OH groups, producing interchain crosslinks, a crosslink density can be expressed as follows: (binding no. of esterification)/(binding no. of esterification and etherification) (see above). The calculated crosslink density was approximately one interchain crosslink per 11 repeat units for EPB-CAA10 and per 16 repeat units for EPTB-CAA10, with these values suggesting that both polymers are gelled.

When the polymers are gelled, the reaction may be very slow and finally may almost cease, thus leading to a conversion saturation. Therefore, the value for the saturated conversion should be closely associated with the degree of branching. The saturated conversion of EPTB-CAA10 is 82–87%, being larger than 75–83% for EPB-CAA10, which can be explained by the difference in reaction rate between the two systems. In fact, the gelling time ( $t_g$ ) is ~60 min for EPTB-CAA10, and ~200 min for EPB-CAA10, as described above.

Figure 7 shows plots of the absorbance of  $\nu(\text{OH})$  and  $\nu_{\text{ester}}(\text{C}=\text{O})$  versus curing time. Both of the absorbances rapidly increase and saturate at about 200 min for EPB-

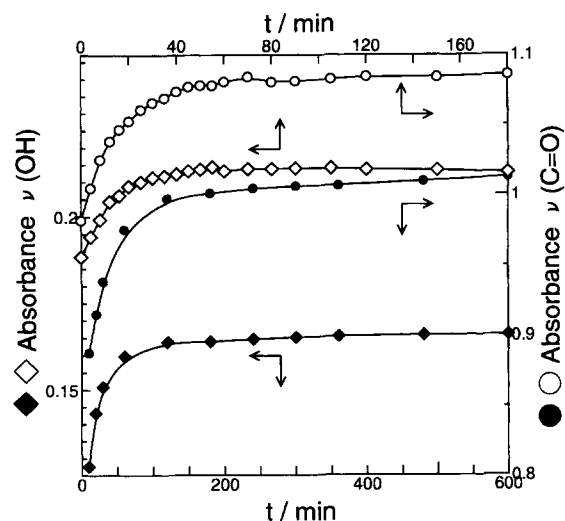


Figure 7 Plots of absorbance of  $\nu(\text{OH})$  and  $\nu_{\text{ester}}(\text{C}=\text{O})$  versus curing time ( $t$ ), where closed symbols represent EPB-CAA10 and open symbols represent EPTB-CAA10: ( $\diamond, \blacklozenge$ )  $\nu(\text{OH})$ ; ( $\circ, \bullet$ )  $\nu_{\text{ester}}(\text{C}=\text{O})$

CDA10 and at approximately 60 min for EPTB-CDA10, which is quite consistent with the values of gelling time obtained from the  $\nu_{\text{COOH}}(\text{C}=\text{O})$  and  $\nu(\text{C}-\text{C})$  bands.

To summarize, in the EPB-CAA10 and EPTB-CAA10 systems a reaction of the epoxide with CAA10 occurs mainly, with a degree of side (branching) reaction of the epoxide with the OH groups being estimated at ~8% for EPB-CAA10 and ~6% for EPTB-CAA10. The gelling time was ~200 min for EPB-CAA10 and ~60 min for EPTB-CAA10.

#### Mesomorphic phase transition

Figure 8 shows d.s.c. curves obtained for the EPB-CAA10 polymers. When  $t$  is 1 or 2 h, the polymer shows two peaks, at ~60 and 90°C during cooling to room temperature after curing at 140°C (1st cooling) and near 70 and 90°C for the subsequent heating run. However, when the prepolymer is cured for 5 h, the lower-temperature peak disappears and there is observed an abrupt change near 45°C, which may be assigned to the  $T_g$ , with one peak existing near 87°C. This thermal behaviour was observed for all of the polymers cured for more than 5 h.

Observations of the texture of EPB-CAA10 were performed under crossed polarizers by the use of an optical microscope. For EPB-CAA10, cured for 1 and 2 h at 140°C, as the temperature was increased, a 'sandy' texture, reminiscent of a smectic phase, appeared near 70°C and disappeared near 90°C, and the polymers were seen to flow by pressing a cover glass of the preparation in the mesophase between 70 and 90°C. On the other hand, after curing for 5 h, the sample became slightly vaguely lighter below 87°C, but no sand-like texture was seen. These results suggest that EPB-CAA10 has a mesophase between 70 and 90°C, reminiscent of a smectic phase, for  $t \leq 2$  h, while when  $t > 5$  h, it has a crystalline region, whose melting corresponds to the peak at ~87°C in the d.s.c. curve (Figure 8), but no mesophase.

Figure 9 shows the temperature dependence of the X-ray diffraction intensity–Bragg angle ( $2\theta$ ) curve for EPB-CAA10. For the  $t = 2$  h polymer, at room temperature, the curves show peaks at values of  $2\theta$  of 3.84,

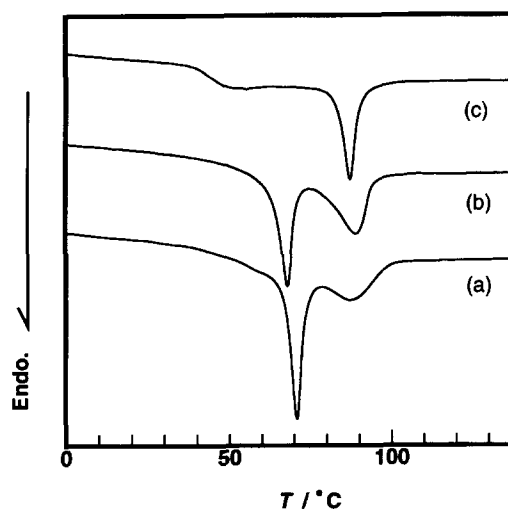


Figure 8 D.s.c. curves of EPB-CAA10 obtained during the heating process after curing at 140°C for various times: (a) 1; (b) 2; (c) 5 h

5.78, 20.32, and 22.84°, corresponding to Bragg spacings of 22.99, 15.78, 4.34, and 3.88 Å, respectively. The wide-angle peaks at 20.32 and 22.84° are assigned to the diffraction peaks from the 110 and 200 reflections of the polyethylene crystalline region. The low-angle peaks at 3.84 and 5.78° may be connected with a smectic layered structure. The molecular shapes and sizes (in the extended state) are shown for the EPB, EPTB and CAA10 monomers in Figure 10. At present, we are unable to understand the low-angle peaks (Bragg spacings of 22.99 and 15.78 Å) from the molecular length of EPB and CAA10, but we could assign the low-angle peaks to higher-order reflections of a layered structure. As the temperature increases, the wide-angle peaks are considerably suppressed between 50 and 75°C, and at 75°C only a broad peak is observed, while the two low-angle peaks are weakened, but still remain at 75°C where the Bragg spacings were 21.75 and 14.72 Å for the low-angle peaks. At a temperature of 100°C above the higher d.s.c. peak (90°C), the wide-angle peaks are much broader, and the low-angle peaks disappear. In EPB-CAA10 which has been cured for 12h, the low-angle peaks are not observed, even at room temperature, and only a broad peak is seen at  $2\theta \sim 20^\circ$ . Therefore, the cured EPB-CAA10 is crystalline, as indicated from the d.s.c. and texture observations, but the degree of crystallinity may be lowered by gelation.

These X-ray diffraction results well explain the mesomorphic phase transition behaviour observed in the texture observations. In Figure 9c, X-ray diffraction intensity versus  $2\theta$  curves are shown for the polymer which has been annealed by cooling the fully gelled polymer ( $t = 12$ h, Figure 9b) at a slow rate of  $1^\circ\text{Cmin}^{-1}$  from 140°C. At room temperature, rather interestingly, the two low-angle peaks are seen again and the wide-angle peaks become somewhat sharper, compared with that of the fully gelled polymer ( $t = 12$ h), and the low-temperature peak near 70°C reappears in the d.s.c. curves. The variation of the low-angle peaks with temperature is almost the same as that of the  $t = 2$ h polymer (Figure 9a), and these disappear at 110°C.

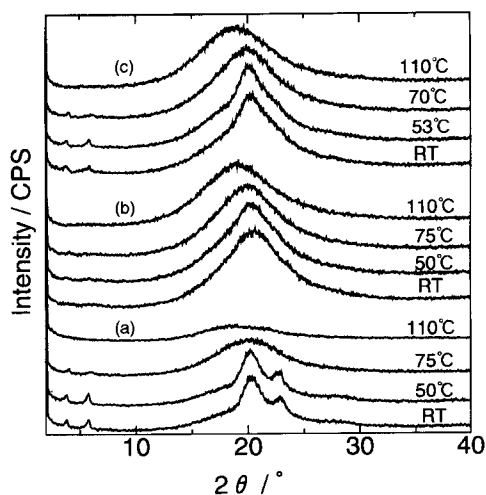


Figure 9 Temperature dependence of the X-ray diffraction intensity–scattering angle ( $2\theta$ ) curves for EPB-CAA10: (a)  $t = 2$ h; (b)  $t = 12$ h; (c) annealed sample after curing for 12h

The mesomorphic phase transition behaviour of EPB-CAA10 appears to be closely associated with gelation. For the shorter reaction time (3.3h), i.e. below the  $t_g$ , EPB-CAA10 has a mesophase reminiscent of a smectic phase between 70 and 90°C. For a longer curing time, i.e. above the  $t_g$ , on the other hand, EPB-CAA10 forms a network structure which is intermolecularly crosslinked, but is still crystalline. However, the crosslinks may disturb the intermolecular ordering and lock in any movement of the main chains, thus leading to the disappearance of the mesophase. In the EPB-CAA10 system, however, a mesophase could be reconstructed, even for the fully gelled polymers, by annealing.

In our preceding paper<sup>13</sup>, we gave a preliminary report of our mesomorphic phase transition studies of the EPTB-CAA10 systems. The d.s.c. curves of EPTB-CAA10 are shown for the heating process in Figure 11, where time (min) in the figure is the total holding time ( $t_h$ ) at 140°C for the prepolymer in a d.s.c. pan; for example, the  $t_h = 25$  min curve represents the 2nd heating run for the polymer cured at 140°C for 5 min in the 1st heating run ( $t_h = 20$  min). The latter curve shows two peaks near 67° (P1) and 87°C (P3). As  $t_h$  increases, the P1 peak shifts to lower temperatures and decreases in intensity, and the P3 peak also decreases, while a new peak (P2) and a  $T_g$  appear at  $\sim 80$  and 45°C, respectively, when  $t_h > 35$  min. Polarizing microscopy observations

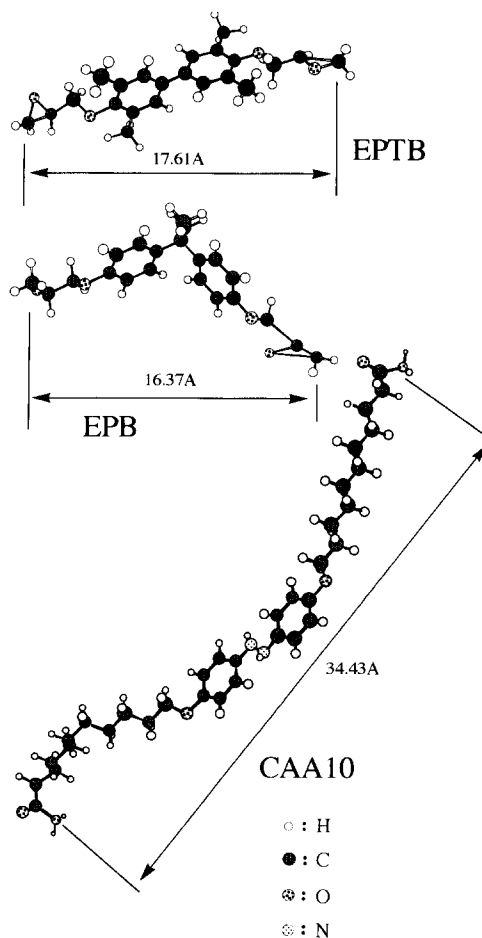
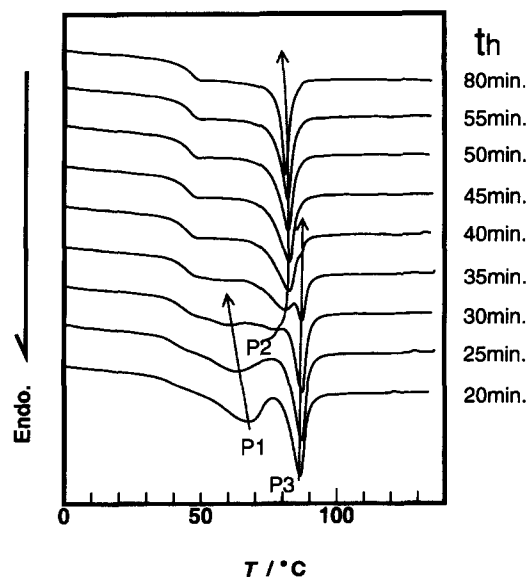


Figure 10 Molecular shapes and dimensions of the EPB, EPTB and CAA10 monomers

under crossed polarizers were made for EPTB-CDA10. When  $t_h = 20$  min, a 'sandy' texture reminiscent of a smectic phase was observed at temperatures between the P1 and P2 peaks, but as the reaction propagates this mesophase is suppressed and a schlieren texture reminiscent of a nematic phase begins to appear, for example from  $t_h = 30$  min. The nematic-like mesophase was observed in the temperature range from  $T_g$  (42°C) to P2 (82°C) in Figure 11, when  $t_h = 50$  min.

In Figure 12, the temperature dependence of the X-ray diffraction intensity versus  $2\theta$  curves for EPTB-CAA10 are shown. When  $t = 20$  min below the  $t_g$ , at room temperature, the polymer has two low-angle peaks at  $2\theta \approx 3.80$  and  $5.82^\circ$  (Bragg spacings of 23.23 and 15.173 Å, respectively) and two wide-angle peaks at  $2\theta$  20°. These low-angle peaks still exist at 70°C but disappear at 100°C, which indicates that the low-angle peaks disappear at 88°C (see Figure 9). On the other hand, as seen in Figure 12b, the fully gelled EPTB-CAA10 ( $t = 12$  h) shows no low or wide-angle peaks, independent of the temperature. These X-ray results support the mesomorphic phase transitions observed in the d.s.c. experiments and from texture observations, where the ungelated polymer shows a smectic-like phase between 65 and 88°C and the gelling polymer shows a nematic-like phase between 45 and 85°C. Interestingly, the low-angle peaks are not reconstructed by cooling the gelling polymer at a slow rate of  $1^\circ\text{C min}^{-1}$  from 140°C (see Figure 12c). This result is inconsistent with that of EPB-CAA10, which might result from the shape of the diepoxide, i.e. the shape of the EPB molecule is bent, while the EPTB molecule is linear (see Figure 10). In EPTB-CAA10, the smectic-like mesophase is observed when  $t < 60$  min ( $t_g$ ), while when  $t$  is larger than  $t_g$ , a nematic-like mesophase appears. It is noted that EPB-CAA10 has a nematic-like mesophase, even when the polymer is fully cured ( $t \gg t_g$ ).



**Figure 11** D.s.c. heating curves of EPTB-CAA10 for different holding times at 140°C, where  $t_h$  is the total holding time for the prepolymer at 140°C in a d.s.c. pan; e.g. the curve of  $t_h = 25$  min is for the polymer sample cooled to room temperature after holding the  $t_h = 20$  min sample at 140°C for 5 min (see text for details)

#### Thermal expansion

Figure 13 shows plots of specific volume ( $v$ ) and thermal expansion coefficient ( $\alpha$ ) versus temperature for EPB-CAA10 and EPTB-CAA10. In EPB-CAA10 for  $t = 2$  h below the  $t_g$  (3.3 h), two abrupt changes are observed near 70 and 90°C, corresponding to the low- and high-temperature d.s.c. peaks, respectively. The gelling EPB-CAA10 polymer ( $t = 12$  h) shows a  $T_g$  near 35°C and an abrupt change near 85°C, while a gelling EPTB-CAA10 for  $t = 12$  h shows a  $T_g$  near 40°C,

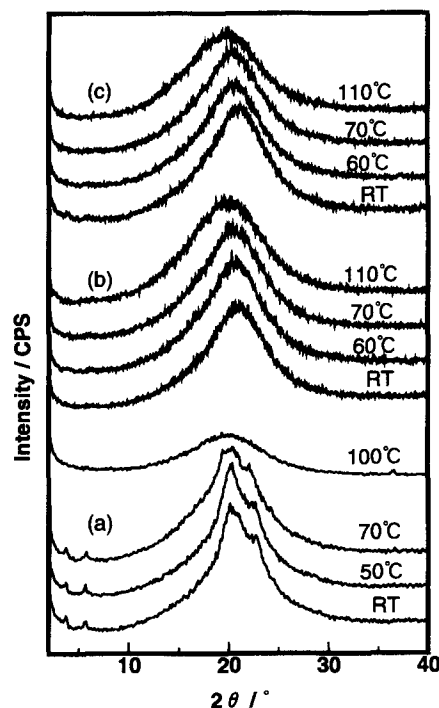


**Figure 12** Temperature dependence of the X-ray diffraction intensity-scattering angle ( $2\theta$ ) curves for EPTB-CAA10: (a)  $t = 20$  min; (b)  $t = 12$  h; (c) polymers annealed by cooling the  $t = 12$  h polymer at a slow rate of  $1^\circ\text{C min}^{-1}$  from 140°C

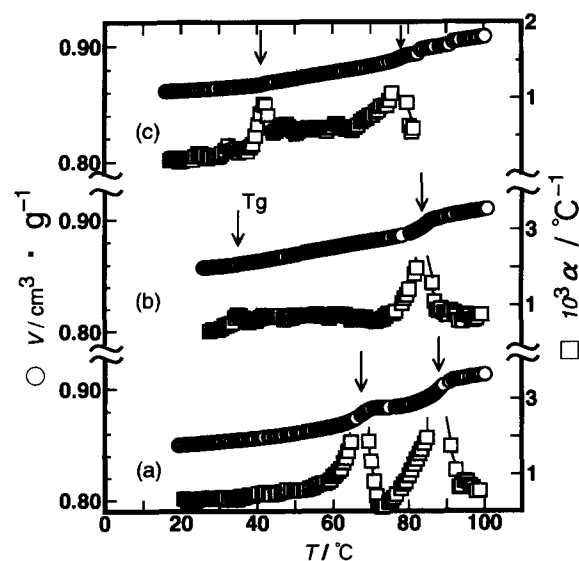


**Figure 13** Plots of specific volume ( $\circ$ ) and thermal expansion coefficient ( $\square$ ) versus temperature: (a) EPB-CAA10 ( $t = 2$  h); (b) EPB-CAA10 ( $t = 12$  h); (c) EPTB-CAA10 ( $t = 12$  h)

**Table 2** Values of the thermal expansion coefficient ( $\alpha$ ) for the gelling EPB-CAA10 and EPTB-CAA10 systems for a hardening time of 12 h

Sample	Thermal expansion coefficient ( $10^{-4} \text{ } ^\circ\text{C}^{-1}$ )	
	$\alpha_1$ , below $T_g$	$\alpha_2$ , above $T_g$
EPB-CAA10	3.4	6.9
EPTB-CAA10	2.1	6.0

and an abrupt change near  $80^\circ\text{C}$ . This phase transition behaviour is also consistent with the d.s.c. data. In Table 2, thermal expansion coefficients are listed for the gelling EPB-CAA10 and EPTB-CAA10 systems. The values of  $\alpha_1$  (below the  $T_g$ ) are  $3.4$  and  $2.1 \times 10^{-4} \text{ } ^\circ\text{C}^{-1}$  for the gelling EPB-CAA10 and EPTB-CAA20 polymers, respectively. These values are somewhat low, but fall within the normal range of thermal expansion coefficients for common epoxy resins above. As already described, the molecular shape of the monomer is considered to be almost linear for the EPTB monomer but bent for the EPB monomer. The smaller value of  $\alpha$  for EPTB-CAA10, compared to EPB-CAA10, could be explained by the shape of the monomer.

## CONCLUSIONS

Two epoxy resins, EPB-CAA10 and EPTB-CAA10, cured by a mesogenic hardening compound, 4,4'-bis( $\omega$ -carboxydecanoxy)azoxybenzene (CAA10) were prepared, and their hardening procedures and mesomorphic phase transitions were investigated. The gelling times ( $t_g$ s) for the prepolymers were determined to be  $\sim 200$  min for EPB-CAA10 and  $\sim 60$  min for EPTB-CAA10 at  $140^\circ\text{C}$ . EPB-CAA10 shows a smectic-like mesophase between  $70$  and  $90^\circ\text{C}$  when the curing time ( $t$ ) at  $140^\circ\text{C}$  is smaller than  $t_g$  but no mesophase when  $t > t_g$ , while EPTB-CAA10 has a smectic-like mesophase between  $60$  and  $87^\circ\text{C}$  when  $t < t_g$ , but a nematic-like mesophase between  $T_g$  ( $50^\circ\text{C}$ ) and  $85^\circ\text{C}$  when  $t > t_g$ . Thermal expansion measurements were made for the polymers. Specific volume-temperature plots showed

abrupt changes near the phase transition temperatures which correspond to those observed by d.s.c. The thermal expansion coefficients were estimated to be  $\sim 3.4 \times 10^{-4} \text{ } ^\circ\text{C}^{-1}$  below  $T_g$  for the gelled EPB-CAA10 ( $t = 12$  h) and  $\sim 2.1 \times 10^{-4} \text{ } ^\circ\text{C}^{-1}$  below  $T_g$  for the gelled EPTB-CAA10 ( $t = 12$  h).

In this present work, we have developed a new class of LC epoxy resins functionalized with mesogenic compounds, namely EPB-CAA10 and EPTB-CAA10. These experiments suggest that it is worthwhile to develop new LC epoxy resins by using mesomorphic hardening compounds.

## REFERENCES

- 1 Broer, D. J., Finkelmann, H. and Kondo, K. *Makromol. Chem.* 1988, **189**, 185
- 2 Broer, D. J., Hikmet, R. A. M. and Challa, G. *Makromol. Chem.* 1989, **190**, 3201
- 3 Broer, D. J., Bover, J., Mol, G. N. and Challa, G. *Makromol. Chem.* 1989, **190**, 2255
- 4 Kirchmeyer, S., Karbach, A., Muller, H., Merer, H. and Dhein, R. *Angew. Makromol. Chem.* 1991, **185/186** 33
- 5 Robinson, A. A., McNamee, S. G., Freidzon, Y. S. and Ober, C. K. *Am. Chem. Soc. Div. Polym. Chem. Polym. Prepr.* 1993, **34**, 743
- 6 Broer, D. J., Lub, J. and Mol, G. N. *Macromolecules* 1993, **26**, 1244
- 7 Carfaagna, C., Amendola, E. and Giamberini, M. *Liq. Cryst.* 1993, **13**, 571
- 8 Lin, O., Yee, A. F. and Sue, H. *Polymer* 1994, **35**, 2679
- 9 Jahromi, S. *Macromolecules* 1994, **27**, 2804
- 10 Jahromi, S., Lub, J. and Mol, G. W. *Polymer* 1994, **35**, 622
- 11 Jahromi, S., Kuipers, W. A. G., Norder, B. and Mijs, W. J. *Macromolecules* 1995, **28**, 2201
- 12 Szczepaniak, B., Frisch, K. C., Perczek, P., Leszczynska, I., Cholinska, M., and Rundnik, E. *J. Polym. Sci. Polym. Chem. Edn* 1995, **33**, 1275
- 13 Osada, S., Tsunashima, K., Inoue, T. and Yano, S. *Polym. Bull.* 1995, **35**, 505
- 14 Lee, H. and Neville, K. *Handbook of Epoxy Resins*, McGraw-Hill, New York, 1967.
- 15 Begnin, A., Billard, J., Bonamy, F., Buisine, J. M., Cuvelier, P. and Du Bois, J. C. *Mol. Cryst. Liq. Cryst.* 1984, **115**, 222
- 16 Ivanov, Y. D., Makarov, S. G. and Iharov, V. Y. *Vibrational Spectrosc.* 1993, **5**, 175
- 17 Alvey, F. B. *J. Polym. Sci.* 1969, **7**, 2117